PREPARED FOR THE U.S. DEPARTMENT OF ENERGY,
UNDER CONTRACT DE-AC02-76CH03073

PPPL-3709
UC-70

PPPL-3709

Results of NSTX Heating Experiments

by

D. Mueller, M. Ono, M.G. Bell, R.E. Bell, et al.

June 2002

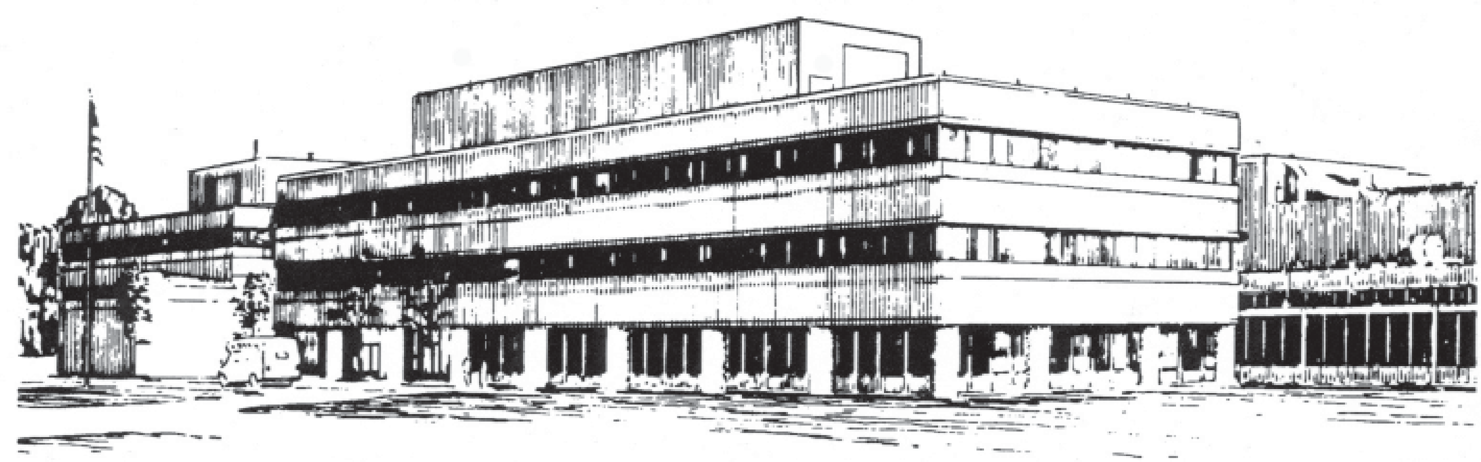

PRINCETON PLASMA PHYSICS LABORATORY
PRINCETON UNIVERSITY, PRINCETON, NEW JERSEY

Results of NSTX Heating Experiments*

D. Mueller M. Ono, M.G. Bell, R.E. Bell, M. Bitter, C. Bourdelle, D.S. Darrow, P.C. Efthimion, E.D. Fredrickson, D.A Gates, R.J. Goldston, L.R. Grisham, R.J. Hawryluk, K.W. Hill, J.C. Hosea, S.C. Jardin, H. Ji, S.M. Kaye, R. Kaita, H.W. Kugel, D.W. Johnson, B.P. LeBlanc, R. Majeski, E. Mazzucato, S.S. Medley, J.E. Menard, H.K. Park, S.F. Paul, C.K. Phillips, M.H. Redi, A.L. Rosenberg, C.H. Skinner, V.A. Soukhanovskii, B. Stratton, E.J Synakowski, G. Taylor, J.R. Wilson, S.J. Zweben, *Princeton Plasma Physics Laboratory,P.O. Box 451, Princeton, NJ, 08543*
Y-K.M. Peng, R. Barry, T. Bigelow, C.E. Bush, M. Carter, R. Maingi, M. Menon, P.M. Ryan, D.W. Swain, J. Wilgen, *Oak Ridge National Laboratory, TN, USA*
S.A. Sabbagh, F. Paoletti, J. Bialek, W. Zhu, *Columbia Univ., NY, USA*
R. Raman, T.R. Jarboe, B.A Nelson, *Univ. of Washington, WA, USA*
R.J Maqueda, G.A. Wurden, *Los Alamos National Laboratory, NM, USA*
R. Pinsker, M. Schaffer, J. Ferron, L. Lao, *General Atomics, CA, USA*
D. Stutman, M. Finkenthal, *Johns Hopkins Univ., MD, USA*
W. Wampler, *Sandia National Laboratory, NM, USA*
S. Kubota, W.A. Peebles, M. Gilmore, *UC Los Angeles, CA, USA*
T.K. Mau, *UC San Diego, CA, USA*
K.C. Lee, C.W. Domier, B. H. Deng, M. Johnson and N. C. Luhmann, Jr., *UC Davis, CA, USA*
P. Bonoli, A. Bers, A. Ram, *MIT, MA, USA*
R. Akers, *EURATOM/UKAEA Lab., Culham, UK*
Y. Takase, A. Ejiri, Y. Ono, S. Shiraiwa, *Univ. Tokyo, Tokyo, Japan*
N. Nishino, *Hiroshima Univ., Hiroshima, Japan*
O. Mitarai, *Kyushu Tokai Univ., Kumamoto, Japan*
M. Nagata, *Himeji Inst. Technology, Hyogo, Japan*
J. G. Yang, H. Na, *Korea Basic Science Institute, Taejeon, Korea*
D. Pacella, ENEA, Frascati, Italy

* Supported by USDOE Contract No. DE-AC02-76CH03073

ABSTRACT

The National Spherical Torus Experiment (NSTX) at Princeton is designed to assess the potential of the low-aspect-ratio spherical torus concept for magnetic plasma confinement. The plasma has been heated by up to 5 MW of neutral beam injection, NBI, at an injection energy of 90 keV and up to 6 MW of high harmonic fast wave, HHFW, at 30 MHz. NSTX has achieved β_T *of 32%. A variety of MHD phenomena have been observed to limit* β*. NSTX has now begun addressing* τ_E *scaling,* β *limits and current drive issues. During the NBI heating experiments, a broad* T_i *profile with* T_i *up to 2 keV,* $T_i > T_e$ *and a large toroidal rotation. Transport analysis suggests that the impurity ions have diffusivities approaching neoclassical. For L-Mode plasmas,* τ_E *is up to two times the ITER-89P L-Mode scaling and exceeds the ITER-98pby2 H-Mode scaling in some cases. Transitions to H-Mode have been observed which result in an approximate doubling of* τ_E

after the transition in some conditions. During HHFW heating, $T_e > T_i$ and T_e up to 3.5 keV were observed. Current drive has been studied using coaxial helicity injection (CHI), which has produced 390 kA of toroidal current and HHFW, which has produced H-modes with significant bootstrap current fraction at low I_p, high q and high β_p.

INTRODUCTION

The National Spherical Torus Experiment (NSTX) is a national collaboration whose goal is to examine stability, confinement and current drive issues in a low aspect ratio magnetic confinement toroidal device.[1] NSTX has a major radius (R) of 0.85 m, minor radius (a) of 0.68 m, aspect ratio, $R/a \geq 1.27$ and elongation (κ) < 2.. The maximum toroidal field (B_T) is 0.6 T and plasma current (I_p) of 1.5 MA has been achieved. For heating the plasma, up to 5 MW total of neutral beam injection (NBI) power is available from 3 co-injecting sources at 90 keV and up to 6 MW of high harmonic fast wave (HHFW) power at 30 MHz can be coupled to the plasma through a 12-strap. Copper plates close to the plasma inside the vacuum vessel suppress magnetohydrodynamic instabilities. The components that are subject to plasma contact during high power operation are protected by a combination of graphite and carbon fiber composite tiles. The HHFW antennas have carbon Faraday shields and boron nitride insulators designed to safely handle the heat load of plasma operation and protect the antennas. The vacuum vessel is capable of a high temperature bake; the center stack can be heated to 350 °C by resistive heating and the passive plates are heated by to about 330 °C by flowing high-pressure helium. The temperature of the outer vessel is controlled with a He gas flow at < 150 °C to maintain acceptable stresses in the vacuum vessel and its appendages. The use of surface boronization by a glow discharge in a mixture of deuterated trimethylboron gas and helium has been effective in reducing the oxygen impurities during subsequent plasma operation.[2]

RESULTS

During NBI heating experiments, the central T_i rises up to 2 keV as measured by charge-exchange recombination spectroscopy (CHERS)[3]. CHERS, which currently has 17 spatial channels and averages data over 20 ms windows, also indicates that there is a large, broad toroidal rotation velocity of up to 240 km/s. During NBI heating, T_e, which is measured by a 60 Hz, 20 spatial channel Thomson scattering system, is lower and more peaked than T_i.[4] The plasma kinetic energy determined from magnetic diagnostics alone[5] agrees well calculations based on the kinetic measurements assuming classical thermalization of the beam-injected ions.

The initial confinement studies on NSTX indicate that, during NBI, the energy confinement time (τ_E) of plasmas which do not undergo a transition to the H-mode is up to twice the conventional ITER L-mode scaling prediction ITER-89p[6] and is reasonably well-matched by the ITER-98pby2 H-mode scaling. Analysis of the plasma transport based on the measured profiles suggests that the ion thermal transport is very low and approaches the neoclassical level. Low particle diffusivity for neon impurity ions injected into the plasma edge has also been measured. The 32 chord horizontal ultra soft x-ray and

16 chord vertical ultra soft x-ray arrays have been used to measure the diffusion of neon puffed into plasmas. Modeling of the differences[7] in the soft x-ray chordal emission profiles between shots with and without neon puffing indicate that there is little neon penetration into the core of the plasma until the occurrence of MHD events. Modeling suggests neon diffusivities < 1 m^2/s, which approaches the neoclassical level, consistent with low ion transport[6] and supporting the high τ_E results. Microstability analysis done with the gyrokinetic code GS2[8] is consistent with the experimental observations of low ion transport. Indeed they show that no Ion Temperature Gradient modes are destabilized for r/a<0.7 (whereas Electron Temperature Gradient modes are destabilized at these radii consistent with a robust inferred electron transport).

H-modes have been observed on NSTX.[9] Figure 1 compares L-mode and H-mode discharges with otherwise similar parameters. The stored energy increases up to a factor of 2 during the H-mode compared to L-mode. A variety of relaxation phenomena have been observed during H-mode periods. Figure 2 shows the time evolution of the deuterium Balmer-α line (D_α) emission, stored energy and H-factor (the energy confinement enhancement over the ITER98pby2 scaling) for 4 discharges. The frequency and magnitude of the D_α signal fluctuations have an effect on the plasma performance. The larger fluctuations correlate with clamped or even reduced plasma stored energy (W_{TOT}). Experiments to study the parametric dependence of the H-mode and its effect on plasma performance are in the initial stages.

Table 1. MHD phenomena observed on NSTX.

Instability	Beta limiting
Ideal low-n kink/ballooning modes	Yes, fast
Resistive wall modes	Yes, fast
Neoclassical tearing modes (NTM)	Yes, soft limit
Sawteeth	Can trigger NTM
Compressional Alfven eigenmodes	No
Current driven kinks	At low q
Locked modes	Sometimes

The maximum stable toroidal beta, the ratio of plasma pressure to toroidal magnetic field pressure, $\beta_T = 2\mu_0\langle p\rangle/B_T^2$, is expected to be large at low aspect ratio compared to moderate aspect ratio magnetic confinement devices. β_T = 32 % has been achieved on NSTX. Fig. 3 is a scatter plot of β_N for NSTX discharges. NSTX plasmas have reached volume-average normalized beta, $\beta_N = 10^8\beta_T\, aB_0/I_p$, at or above the theoretical limit for plasmas without the stabilizing effect of a nearby conducting wall, $\beta_N / l_i \sim 6$, as shown in the upper part of Fig. 3. NSTX data indicates that the maximum achievable β_N increases with plasma internal inductance, l_i, similar to the trend observed at conventional aspect ratio. Stability calculations of reconstructed experimental equilibria show that plasmas at the present empirical limit, $\beta_N / l_i \sim 8$ are about 25% about the no-wall beta limit. This can be compared to $\beta_N = 4\ l_i$ for a more conventional aspect ratio tokamak. The lower part of Fig. 3 shows the dependence of β_N on the pressure peakedness, p(0)/<p>. It is clear that broader pressure profiles permit operation at higher β_N, as expected. Near the β limit, a variety of MHD phenomena are observed.[10] Table 1 lists the various instabilities observed in NSTX and indicates whether they cause fast, large reductions in β, if they represent a soft β limit that acts to reduce confinement, or if they appear to have no effect on β. A β collapse frequently occurs in plasmas shortly after the time the n=1 kink and high-n ballooning modes become unstable, as calculated by the DCON[11] code. Resistive wall modes have been observed in experiments when the ideal n=1 no-wall β_N limit was violated at high heating power and sufficiently low plasma rotation, leading to fast beta collapses.[10] Neoclassical tearing Modes (NTM)[12, 13] have been observed on NSTX. These modes are rotating or possibly locked magnetic islands driven by bootstrap current. On NSTX, these modes were more frequently observed prior to realignment of one of the poloidal field coils to reduce its n=1 asymmetry. However, since the bakeout temperature for NSTX was raised in the same period, it is unknown whether it was improved impurity control or better magnetic geometry that reduced the incidence of these modes. The NTMs now occur generally when q(0) falls below 1 and sawteeth oscillations trigger the growth of the modes.. Compressional Alfvén Eigenmodes (CAE)[14] have been observed during NBI heating on NSTX at frequencies well below the ion cyclotron frequency.[15] CAE are compressional waves, like sound waves rather than transverse waves, that can be driven by fast ions. There does not seem to be a NBI power threshold for producing this instability (at least if there is a power threshold, it is below 1 MW on NSTX), instead it is the ion speed relative to the Alfvén speed that is relevant parameter. CAEs appear to have little direct effect on the macroscopic plasma stability or confinement properties.

A critical issue for ST development is reducing reliance on induction from a central solenoid to establish and maintain the plasma current. NSTX is studying a number of methods of non-inductive current drive, including HHFW current drive, the neoclassical bootstrap current, and co-axial injection (CHI). The HHFW system is comprised of a 12-element antenna array with independently controllable phasing of the successive elements to launch waves with a phase velocity suitable for either current drive or heating. The 30 MHz frequency of the system is 10 to 15 times the fundamental ion cyclotron frequency for hydrogen. HHFW power couples predominantly to the electrons. In the heating phasing which produces both co- and counter-directed waves with a parallel wavenumber $k_{||} \approx 14 m^{-1}$, the electrons have been heated up to 3.5 keV with $T_e > T_i$.

By phasing the antenna straps to launch directed waves with $k_{||} \approx 7 m^{-1}$, the phase velocity approaches the electron thermal velocity, creating the possibility for driving current with the RF power. Initial experiments with HHFW current drive have shown changes in the loop voltage required to maintain constant plasma current when the HHFW phasing is changed from co- to counter-. Although the absorption of HHFW waves by thermal ions is small, during NBI heating, HHFWs can also interact with injected energetic ions, this may reduce the current drive efficiency. Figure 4 shows the spectrum from a neutral particle analyzer taken during an HHFW and NBI heated plasma around the time of RF turnoff. The formation of a “tail” on the energy spectrum of particles above the injection energy, 80keV, indicates that acceleration of ions by the HHFW is occurring.

On NSTX, the stainless steel vacuum vessel has insulators at the top and bottom of the machine to prevent poloidal current flow in the vessel, as shown in Figure 5. The inner and outer divertor plates can be biased to initiate a discharge carrying poloidal plasma current. In the presence of a toroidal magnetic field, the plasma develops a toroidal current. This is the process of coaxial helicity injection, CHI, which has been used on smaller machines, the Current Drive Experiment-Upgrade (CDX-U)[16] at Princeton, the Helicity Injected Torus-I (HIT-I),[17] and the Helicity Injected Torus-II (HIT-II)[18] at the University of Washington, to initiate discharges and obtain toroidal current. CHI initially drives a current along open helical field lines. The current profile is expected to be initially hollow and then flatten through magnetic reconnection to fill the volume. In NSTX, the CHI discharge is driven by a 50 kA, 1 kV DC power supply. The discharge begins near the lower, insulator where the gas is injected into the torus. The ΔB^2_{tor}, $J_{pol} \times B_T$ stress across the current layer causes the plasma to move upward into the main torus chamber as can be seen in the TV images in Fig. 5. The poloidal field currents must then be adjusted to maintain equilibrium. Figure 6 illustrates the time evolution of a CHI discharge. Preprogramming of the coil currents was used to control the plasma equilibrium position and maintained position control for up to 350 ms when the discharge was intentionally terminated. Using this technique we have been able to produce stable discharges with 390 kA of toroidal current using 28 kA of injector current. The toroidal current produced by CHI in NSTX is more than an order of magnitude greater than that produced previously in other spherical tori or spheromaks.

SUMMARY

NSTX has begun exploration of the confinement properties of the ST and performed initial current drive experiments. The energy confinement scales better than expected in the L-mode by up to a factor of 2 during NBI. Systematic studies of H-mode confinement are just beginning, but the first results indicate that the confinement is as good or better than the H-mode scaling laws developed from conventional aspect ratio devices. Studies of stability and MHD have identified several modes that may or may not limit plasma performance depending on the type of instability. HHFW has injected significant power into NSTX and produced H-modes with high β_p and significant bootstrap current. CHI has demonstrated the ability to initiate and drive nearly 400kA of toroidal current.

Figure Captions:

Figure 1. Time evolution of the plasma current, neutral beam power, D-α emission and plasma stored energy for two discharges, one (solid) that undergoes a transition from L-mode to H-mode at 0.193 s. Note the change in the stored energy trace between the two discharges at the time of the transition.

Figure 2. Time evolution of D-α,, stored energy, and H-factor, the enhancement over the ITER98pby2 scaling. The frequency of the spikes in the emission D-α increases and their amplitude decreases with increasing NBI power.

Figure 3. Occurrence plot of β_N for NSTX discharges versus a) plasma internal inductance l_i and b) versus pressure peakedness. The values of β_N, l_i and $p(0)/\langle p \rangle$ are from analysis of the magnetic data with the EFIT code.

Figure 4. Energy spectra from the neutral particle analyzer showing the decay in the high-energy tail in the beam ions driven by HHFW after the HHFW is turned off.

Figure 5. a) Schematic of NSTX vacuum vessel showing the relative location of the insulating breaks in the vacuum vessel and the direction of the magnetic and electric fields. b) Plasma TV images of a CHI discharge at 16 and 18 ms as the discharge is allowed to grow vertically and begins to fill the vessel.

Figure 6. Injector current, toroidal current, injector voltage, injector flux and current in a lower poloidal field coil (PF3L) as a function of time for a high current CHI discharge. PF3L current is varied to control the plasma vertical position in an open loop mode.

[1] M. Ono et al., Nucl. Fusion **40**, 557 (2000).

[2] H. W. Kugel, *et al*., Proc. of the 15th International Conference on Plasma Surface Interactions in Controlled Fusion Devices, Gifu, Japan, May 27-31, 2002.

[3] R. Bell et al., 28th EPS Conf. On Contr. Fusion and Plasma Phys, Funchal, 18-22, June 2001, ECA **25A**, 1021 (2001).

[4] D. Johnson, et al., Rev, Sci. Instrum. **70**, 776 (1999).

[5] S. A. Sabbagh, et al., Nucl. Fusion **41**, 1601 (2001).

[6] ITER physics basis 1999 Nucl. Fusion **39**, 2232 (1999).

[7] D. Stutman, et al., 28th EPS Conf. On Contr. Fusion and Plasma Phys, Funchal, 18-22, June 2001, ECA **25A**, 445 (2001).

[8] M. Kotschenreuther, G. Rewoldt and W.M. Tang, Computer Phys. Com., **88**, 128 (1995).

[9] R. Maingi et al., Phys. Rev. Lett., **88**, 035003 (2002).

[10] S. A. Sabbagh et al., Phys. Plasmas, 9, 2085 (2002).

[11] A. H. Glasser and M. S. Chance, Bull Am. Phys. Soc., **42**, 1848 (1997).

[12] Z. Chang, dt al., Phys. Rev. Lett. **74**, 4663 (1995).

[13] D. A. Gates, et al., Nucl. Fus. **37**,1593 (1997).

[14] N. Gorelenkov and C. Cheng, Nucl. Fus. **35**, 1743 (1995).

[15] E.D. Fredrickson, et al., Phys. Rev. Lett.

[16] M. Ono, et al., Phys. Rev. Lett., **44**, 393 (1980).

[17] B. A. Nelson, et al., Phys. Plasmas, **2**, 2337 (1995).

[18] T. R. Jarboe, et al., Phys Plasmas, **5**, 1807 (1998) and T.R. Jarboe, et al., in Fusion Energy 1998 (Proc. 17th Int. Conf. Yokohama, 1998(, IAEA Vienna (2000).

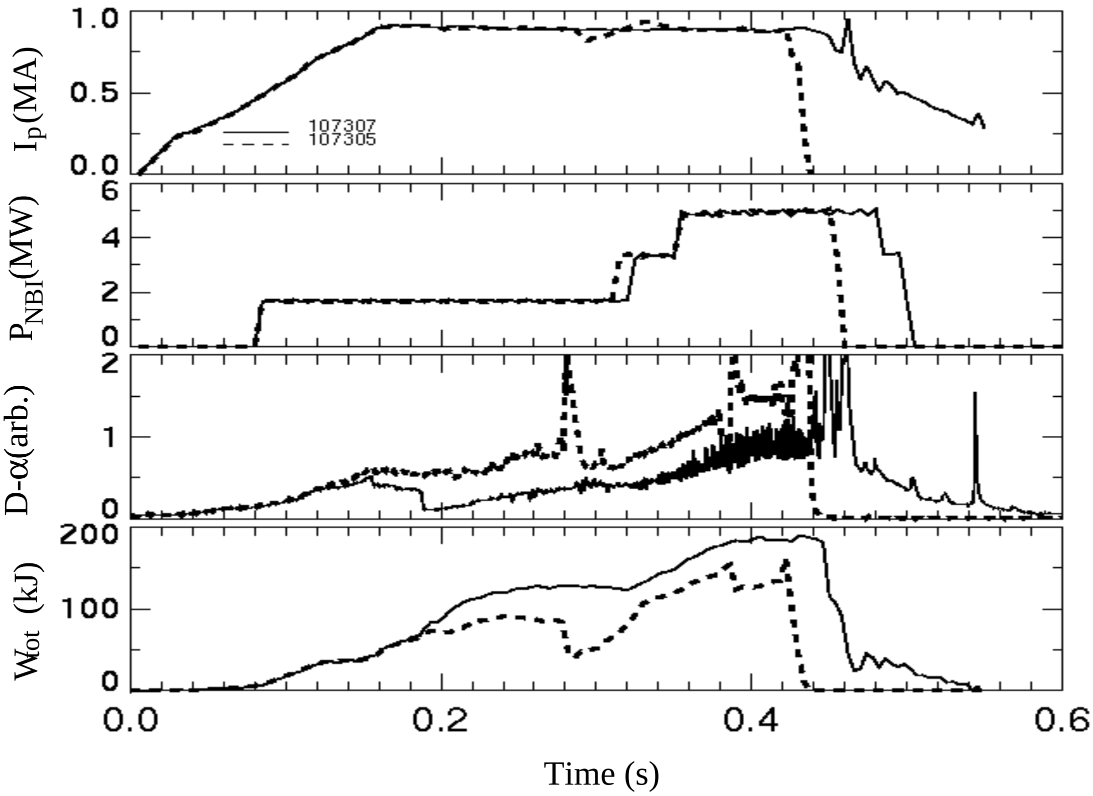

1.0
0.5
0.0
I_p(MA)
107307
107305
6
4
2
0
P_{NBI}(MW)
2
1
0
D-α(arb.)
200
100
0
W_{tot} (kJ)
0.0
0.2
0.4
0.6
Time (s)

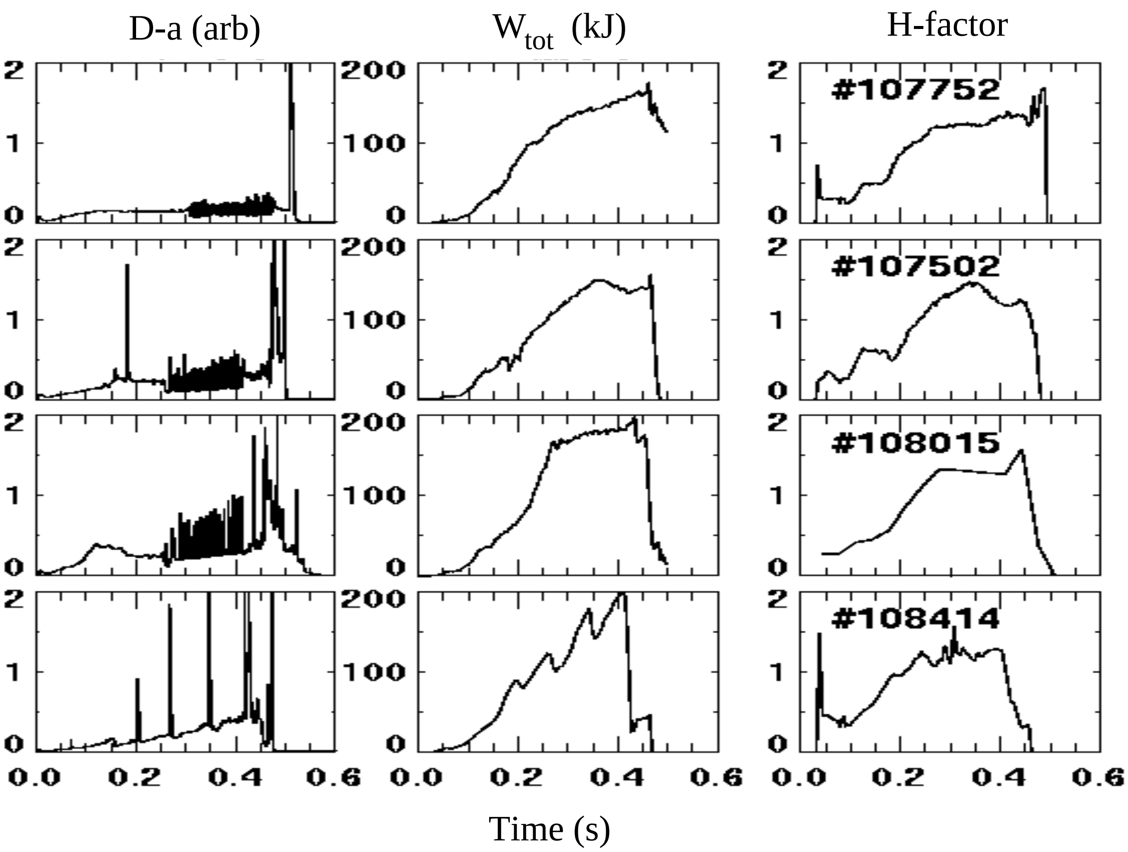
D-a (arb)
W_{tot} (kJ)
H-factor
#107752
#107502
#108015
#108414
Time (s)

(a)

(b)

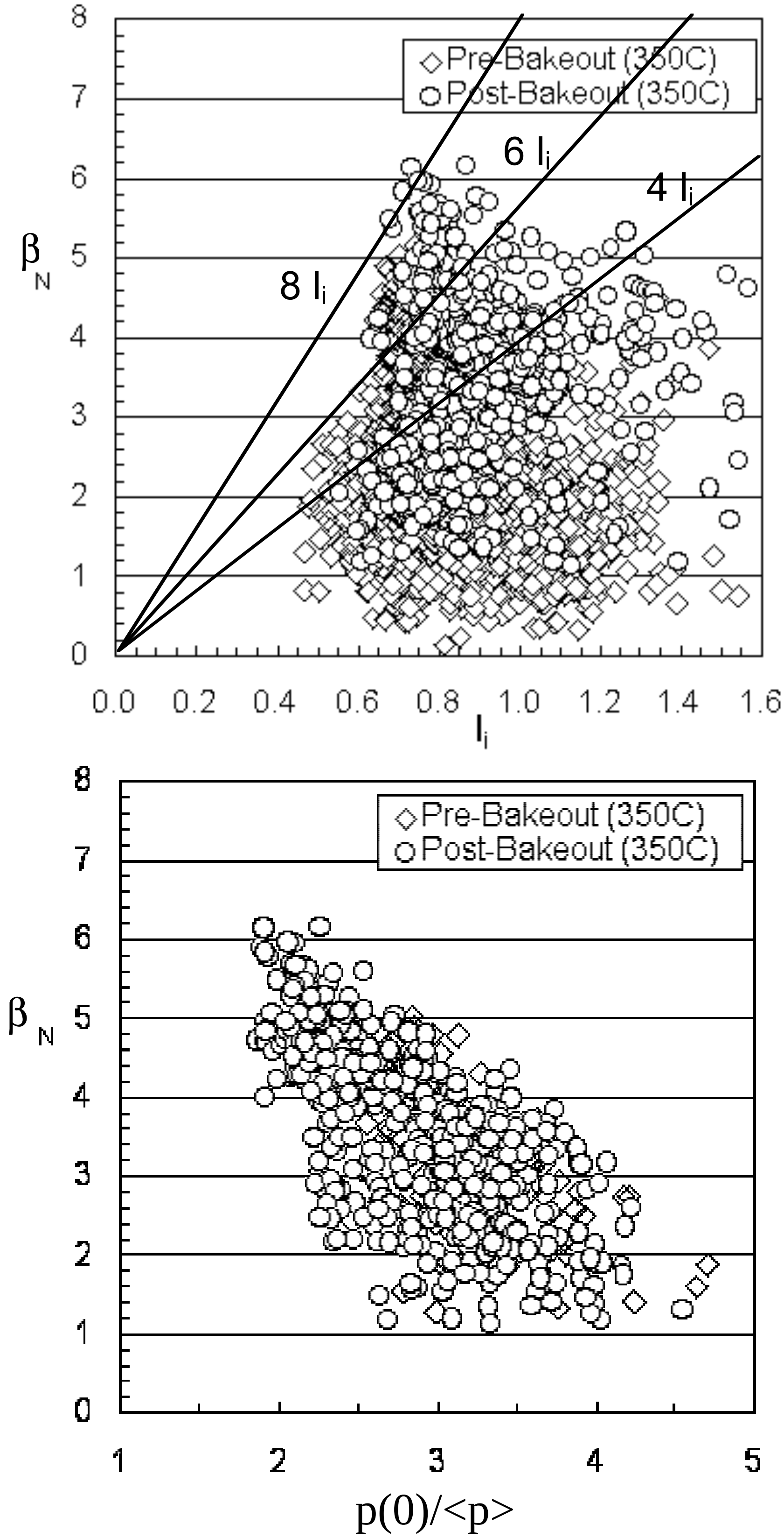

Pre-Bakeout (350C)
Post-Bakeout (350C)
β_N
l_i
8 l_i
6 l_i
4 l_i
0.0 0.2 0.4 0.6 0.8 1.0 1.2 1.4 1.6
0 1 2 3 4 5 6 7 8
Pre-Bakeout (350C)
Post-Bakeout (350C)
β_N
p(0)/<p>
1 2 3 4 5

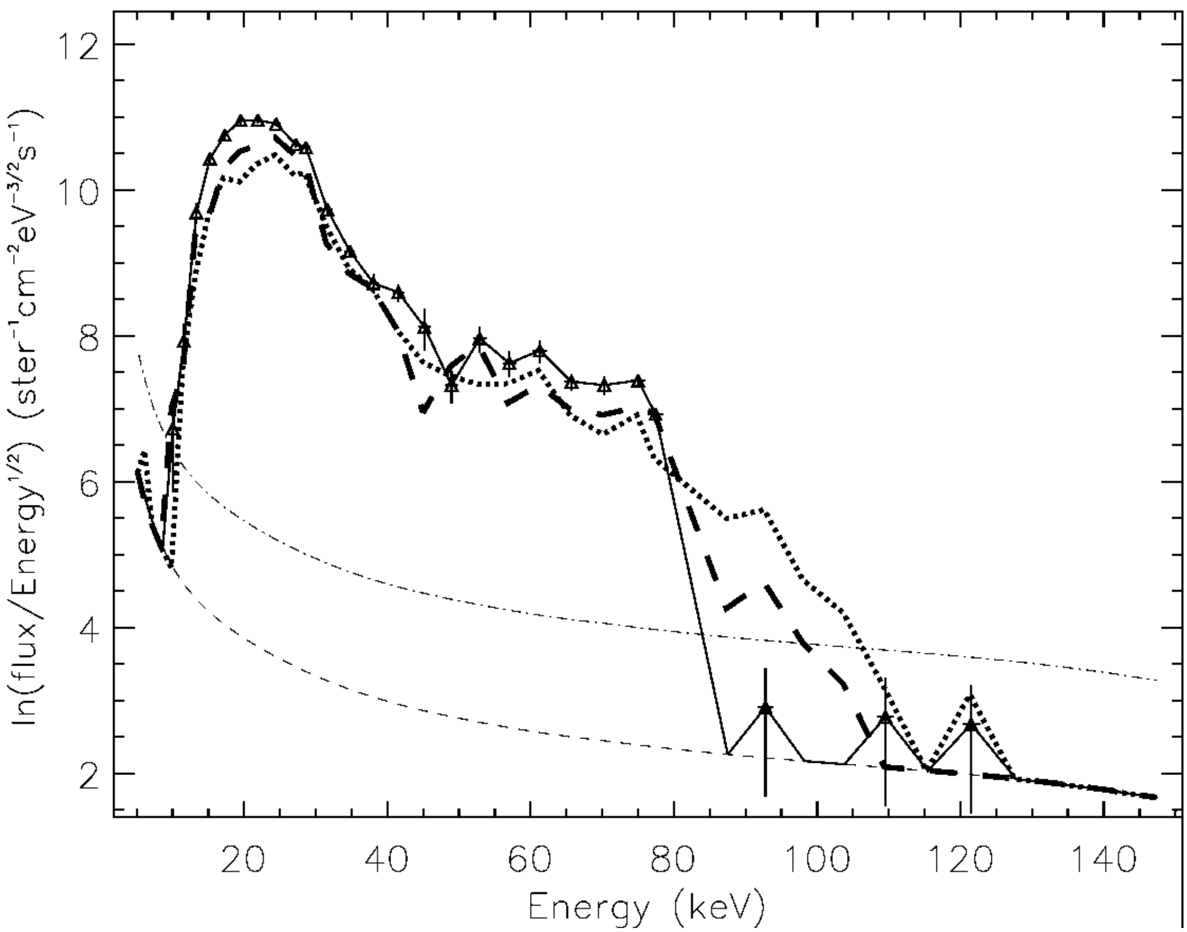

12
10
8
6
4
2
20
40
60
80
100
120
140
Energy (keV)
ln(flux/Energy$^{1/2}$) (ster^{-1}cm^{-2}eV$^{-3/2}$s^{-1})

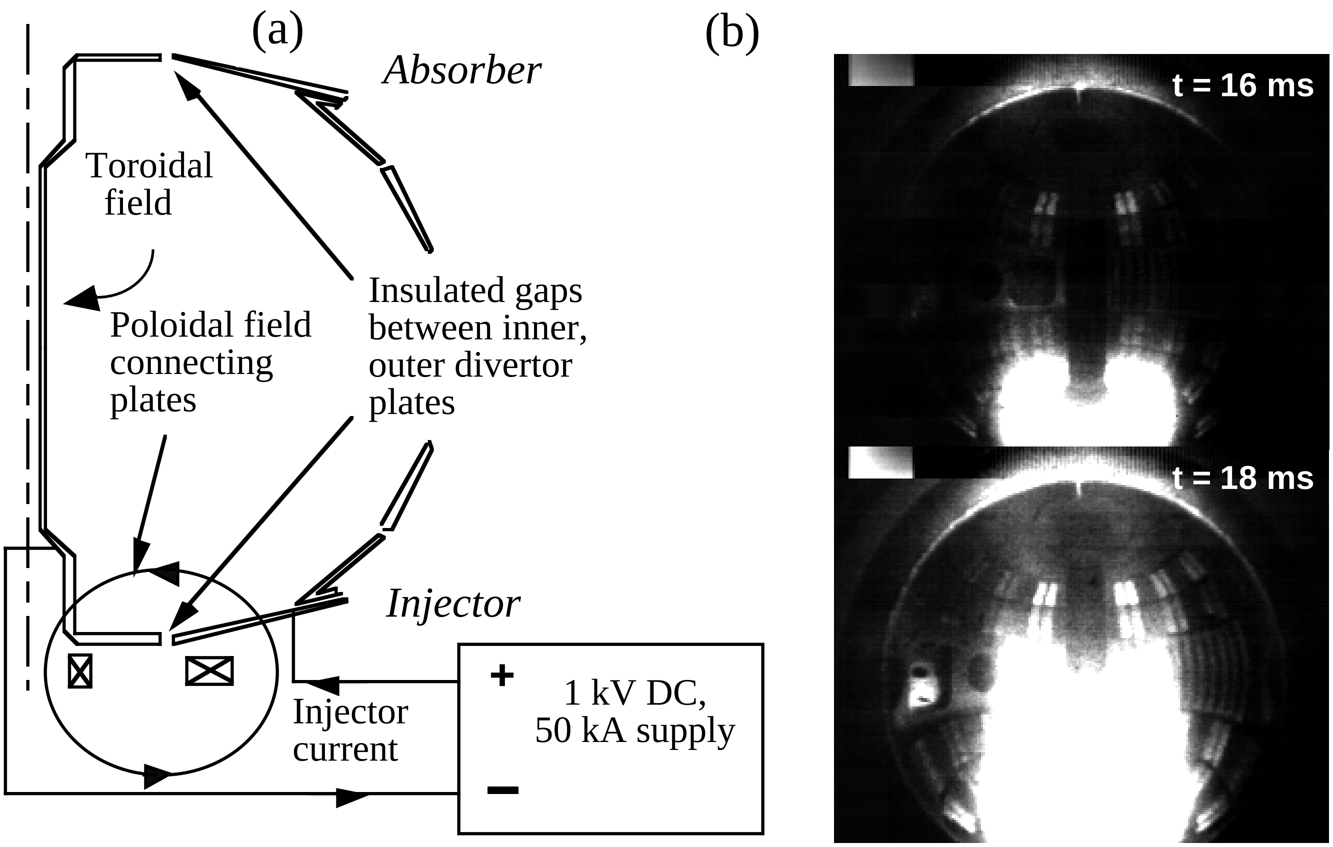
(a)
(b)
Absorber
Toroidal field
Poloidal field connecting plates
Insulated gaps between inner, outer divertor plates
Injector
+
1 kV DC, 50 kA supply
Injector current
–
t = 16 ms
t = 18 ms

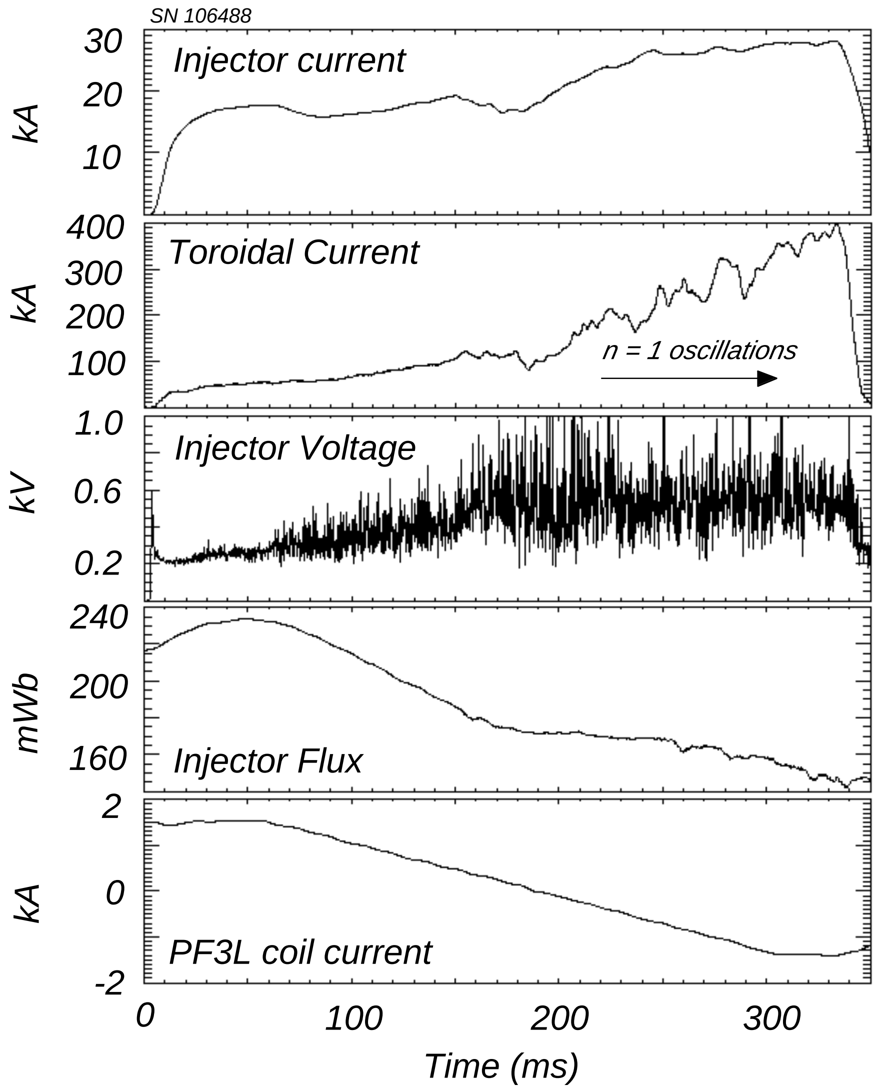

SN 106488
30
20
10
kA
Injector current
400
300
200
100
kA
Toroidal Current
n = 1 oscillations
1.0
0.6
0.2
kV
Injector Voltage
240
200
160
mWb
Injector Flux
2
0
-2
kA
PF3L coil current
0
100
200
300
Time (ms)

External Distribution

Plasma Research Laboratory, Australian National University, Australia
Professor I.R. Jones, Flinders University, Australia
Professor João Canalle, Instituto de Fisica DEQ/IF - UERJ, Brazil
Mr. Gerson O. Ludwig, Instituto Nacional de Pesquisas, Brazil
Dr. P.H. Sakanaka, Instituto Fisica, Brazil
The Librarian, Culham Laboratory, England
Library, R61, Rutherford Appleton Laboratory, England
Mrs. S.A. Hutchinson, JET Library, England
Professor M.N. Bussac, Ecole Polytechnique, France
Librarian, Max-Planck-Institut für Plasmaphysik, Germany
Jolan Moldvai, Reports Library, MTA KFKI-ATKI, Hungary
Dr. P. Kaw, Institute for Plasma Research, India
Ms. P.J. Pathak, Librarian, Insitute for Plasma Research, India
Ms. Clelia De Palo, Associazione EURATOM-ENEA, Italy
Dr. G. Grosso, Instituto di Fisica del Plasma, Italy
Librarian, Naka Fusion Research Establishment, JAERI, Japan
Library, Plasma Physics Laboratory, Kyoto University, Japan
Research Information Center, National Institute for Fusion Science, Japan
Dr. O. Mitarai, Kyushu Tokai University, Japan
Library, Academia Sinica, Institute of Plasma Physics, People's Republic of China
Shih-Tung Tsai, Institute of Physics, Chinese Academy of Sciences, People's Republic of China
Dr. S. Mirnov, TRINITI, Troitsk, Russian Federation, Russia
Dr. V.S. Strelkov, Kurchatov Institute, Russian Federation, Russia
Professor Peter Lukac, Katedra Fyziky Plazmy MFF UK, Mlynska dolina F-2, Komenskeho Univerzita, SK-842 15 Bratislava, Slovakia
Dr. G.S. Lee, Korea Basic Science Institute, South Korea
Mr. Dennis Bruggink, Fusion Library, University of Wisconsin, USA
Institute for Plasma Research, University of Maryland, USA
Librarian, Fusion Energy Division, Oak Ridge National Laboratory, USA
Librarian, Institute of Fusion Studies, University of Texas, USA
Librarian, Magnetic Fusion Program, Lawrence Livermore National Laboratory, USA
Library, General Atomics, USA
Plasma Physics Group, Fusion Energy Research Program, University of California at San Diego, USA
Plasma Physics Library, Columbia University, USA
Alkesh Punjabi, Center for Fusion Research and Training, Hampton University, USA
Dr. W.M. Stacey, Fusion Research Center, Georgia Institute of Technology, USA
Dr. John Willis, U.S. Department of Energy, Office of Fusion Energy Sciences, USA
Mr. Paul H. Wright, Indianapolis, Indiana, USA

The Princeton Plasma Physics Laboratory is operated
by Princeton University under contract
with the U.S. Department of Energy.

Information Services
Princeton Plasma Physics Laboratory
P.O. Box 451
Princeton, NJ 08543

Phone: 609-243-2750
Fax: 609-243-2751
e-mail: pppl_info@pppl.gov
Internet Address: http://www.pppl.gov